

Effect of particle size of KL zeolite supporting Pt catalyst on n-octane aromatization

Trakarnroek, S.¹, Ittisanronnachai, S.¹, Osuwan, S.¹, Rirksomboon, T.¹, Jongpatiwut, S.², and Resasco, D.E.²

¹The Petroleum and Petrochemical College, Chulalongkorn University, Bangkok, Thailand, 10330

²School of Chemical, Biological, and Materials Science, The University of Oklahoma, Norman, OK 73019

©2004 Trakarnroek, S., Ittisanronnachai, S., Osuwan, S., Rirksomboon, T., Jongpatiwut, S., and Resasco, D.E., Prepared for Presentation at 2004 Annual Meeting/AIChE Annual Meeting/November 7-12, Topics in Zeolites, Unpublished, AIChE Shall Not Be Responsible For Statements or Opinions Contained in Papers or Printed in its Publications

Abstract

Ethylbenzene (EB) and xylenes are important raw materials in the petrochemical industry. Pt/KL catalyst is well known for its high activity and selectivity for n-hexane aromatization to benzene. However, for n-octane, most of the products obtained on this catalyst are benzene and toluene which would be undesired secondary reaction products in the selective production of C8-aromatics. In a previous study, we observed that on Pt/KL, n-octane was first aromatized inside zeolite channel producing either EB or o-xylene (OX) which are products predicted by a direct one-six member ring closure. Then, EB and OX would further react on platinum cluster inside the zeolite forming toluene and benzene before escaping zeolite channel. Since the critical size of OX (0.76 nm) is considerably larger than EB (0.67 nm), OX diffuses with greater difficulty leading to a higher chance to undergo secondary reaction than EB. As a result, the variation of the EB/OX ratio can be used to indicate the degree of secondary hydrogenolysis.

In this contribution, we have investigated the effect of zeolite particle size on the product distribution of n-octane aromatization, a series of KL zeolites of varying particle sizes was synthesized using the microwave-hydrothermal treatment technique. The particle sizes of the zeolites were varied by preparing the gel with different ageing times (17-24 hr), amount of barium (100-300 ppm), and amount of seeding. The synthesized zeolites were characterized by several techniques, BET, XRD, SEM, and a particle size analyzer. XRD results demonstrated the high crystallinity of all the zeolites prepared. SEM and particle-size analysis indicated that the average particle size of the zeolites were between 1.0 and 1.8 microns. Pt supported on different zeolite catalysts (Pt/KL) were prepared by vapor phase impregnation (VPI). The fresh catalysts were characterized by DRIFTS of adsorbed CO and hydrogen chemisorption techniques. The results indicated that Pt clusters are well-dispersed inside the zeolite channel for all catalysts. The catalyst prepared from larger zeolite size showed higher fraction of Pt stabilized inside the channel than the catalyst prepared from smaller particle size zeolite. The aromatization of n-octane was tested on the different catalysts at 500°C and atmospheric pressure. It was found that as the zeolite particle size increased the secondary reaction increased resulting in a lower yield of C8-aromatics, especially OX but more benzene and toluene in effluent product. In conclusion, to maximize the selectivity to C8-aromatics, the catalyst with short diffusion path is required.

Keywords: n-octane aromatization, zeolite, microwave-hydrothermal

Introduction

The aromatization of n-alkane is an important reaction to obtain high added-value products from a naphtha feedstock that is abundant in refinery operations. This reaction has many industrial application and can be carried out on both bifunctional (acid-metal) and monofunctional (only-metal) catalysts. The advantage of using monofunctional catalysts is the elimination of the isomerization paths, which typically occur on in the bifunctional catalysts and result in lower selectivity to aromatics. Platinum clusters in alkaline LTL zeolite is the efficient catalyst for the dehydrocyclization of n-hexane into benzene [Meriaudeau and Naccache, 1997]. However, for n-octane aromatization, Pt/KL catalysts are not as effective as for n-hexane aromatization. Although Pt/KL catalyst prepared by vapor phase impregnation (VPI) provided the highest Pt dispersion and maximum incorporation of Pt inside the channels of the zeolite, the activity for n-octane aromatization was still low and quickly dropped after a few hours on stream. The product distribution obtained from the n-octane conversion showed benzene and toluene as the dominant aromatic compounds, with small quantities of ethylbenzene (EB) and o-xylene (OX), which are the expected products from the direct closure of the sixed-member ring. Since the pore size of the KL zeolite is 0.71 nm [Arika et al., 1985], larger than the critical diameter of EB but smaller than that of OX, OX diffuses much slower than EB. As a result, OX would preferential convert to benzene and toluene before escaping from the pore of zeolite. It is suggested that the pore length of the zeolite have a great impact on product distribution and catalyst life [Jongpatiwut et al., 2003].

The idea of short channel KL zeolite has been previously discussed by Treacy [Treacy, 1999] to minimize the problem of Pt entombment due to Pt agglomeration and coking. Furthermore, the small particle size of zeolite provides advantages over larger particle size when used as a catalyst, or catalyst base. In the hydrocarbon conversion reaction, their enhanced ratio of surface area to mass, high diffusion rates and reactivities, and resistance to deactivation by pore plugging and surface contamination [Verduijn et al., 2001]. Many researches have synthesized zeolite KL by conventional hydrothermal treatment. The optimum composition of synthesis gel is 2.62 K₂O:Al₂O₃:10SiO₂:160H₂O. SEM showed the product to be formed solely of well-defined cylindrical crystals having a particle size of 2.0 to 2.5 micron [Wortel et al., 1985]. Addition of small amounts of metal has the effect in suppressing unwanted zeolite W formation and forming smaller or more cylindrical zeolite L particles [Verduijn, 1992]. However, longer crystallization time was used in the conventional hydrothermal treatment, and heat transfer occurring by convection and conduction resulted in the slow increase in temperature. This also leads to temperature gradient. To reduce the crystal size, it is necessary to reduce the temperature, concomitantly, increase the crystallization time. Longer crystallization time not only reduces the crystal size, but also increases the risk of undesirable crystalline material. Employing microwave radiation was introduced and useful in manufacturing of microporous crystalline materials [Chu et al., 1988]. A general advantage of microwave radiation provides small crystal size of crystalline material in shorter crystallization time. Since this method gives higher heating rate due to volumetric heating, resulting in homogeneous nucleation, and fast dissolution of precipitated gels. Furthermore, it is a clean and economical heating system [Romero, 2004].

Therefore, in this contribution, we reported the effect of particle size of KL zeolite on n-octane aromatization. First, KL zeolites were synthesized by using microwave hydrothermal treatment. The effects of ageing time, amount of barium, and seeding on the particle size of zeolite KL were investigated. All synthesized KL zeolites were characterized by using XRD, nitrogen adsorption, SEM, XRF, FT-IR, and dynamic light scattering

spectrometer (DLS). Pt supported on the synthesized KL zeolites were prepared and tested for activity and selectivity of n-octane aromatization 500°C and atmospheric pressure. The fresh catalysts were also characterized by means of FTIR of adsorbed CO to provide the location of Pt particle and hydrogen chemisorption to provide the dispersion of Pt and particle size of Pt. Temperature programmed oxidation (TPO) was also applied to measure amount of coke on the catalysts.

Experimental

Materials

n-Hexane (C₆H₁₄) of min 99% and n-octane (C₈H₁₈) of min 99% purity were obtained from Merck. The commercial catalyst support K-LTL zeolite (HSZ-500, SiO₂/Al₂O₃ = 6, surface area = 280 m²/g) was obtained from Tosoh company, Japan. Platinum (II) acetylacetonate ([CH₃COCH=(CO-)CH₃]₂Pt) was obtained from Alfa Aesar (Wheat Deptford, USA). Colloidal silica (40%wt suspension) was obtained from Aldrich. Potassium hydroxide (KOH) and Barium hydroxide (Ba(OH)₂) were supplied by Carlo Erba reagenti. Aluminium hydroxide (Al(OH)₃) of 99.8% purity was purchased from Merck.

Synthesis of zeolite

The KL zeolites were synthesized from the mixture of silicate and potassium aluminate solutions to get the following composition, 2.65K₂O: 0.0032BaO:0.5 Al₂O₃:10SiO₂:159H₂O. The potassium aluminate solution was prepared by dissolving 2.64 g of Al(OH)₃ in the 8.15 M of KOH solution. The Silicate solution was prepared by mixing colloidal silica with 2.8 mM of Ba(OH)₂ solution and stirring for 15 min. The silicate and aluminate solution were then mixed and stirred vigorously for different periods of ageing time at room temperature. After that, the gel mixture was transferred to a microwave vessel and heated using a MARS5 microwave up to 170°C within 2 min and maintained at such a temperature from 15-30 hr. The resultant material was washed with deionized water until pH 10 and centrifuged to separate the solid phase from the solution. The solid product was dried in an oven at 110°C overnight and calcined at 500°C in the flowing air.

Characterization of synthesized KL zeolite

1 *X-Ray diffractometer (XRD)* : The zeolite structures of synthesized KL zeolites were characterized using a Rigaku X-Ray Diffractometer, with Cu K line as incident radiation and a filter at a scanning rate of 5 °/s.

2 *Scanning electron microscope (SEM)* : The crystal morphology was studied using a JEOL 5200-2AE scanning electron microscope.

3 *X-Ray fluorescence spectroscope (XRF)* : The Si/Al ratio was measured by an SRS 3400 Bruker X-Ray fluorescence spectroscope, with 99.8% boric acid as binder.

4 *Dynamic light scattering (DLS) or photon correlation spectroscopy (PCS) measurements* : DLS was used to determine the average particle size using Malvern 4700 spectrometer equipped with Ar-ion laser as a light source. The detector was fixed at 60° with respect to incident beam direction. The photomultiplier aperture used was 150 μm.

5 *BET surface area measurements* : Nitrogen adsorption was employed to analyze the surface area and pore volume of synthesized KL zeolites. The adsorption isotherms were collected at 77K using a Thermo Finnigan sorptomatic modeled 1100 series.

Catalyst Preparation

Pt/KL catalysts were prepared by vapor phase impregnation (VPI). Prior to impregnation, the support was dried at 110°C overnight and calcined at 500°C in a dry air flow of 100 cm³/min.g for 5 hr.

The Pt/KL catalyst was prepared by physical mixing the desired amount of platinum (II) acetylacetonate (Alfa Aesar) and the dried support under nitrogen atmosphere. The mixture was then loaded in a tube reactor under helium flow of 5 cm³/min.g. The mixture was slowly heated to 40°C and held there for 3 hr, and ramped again to 60°C and held for 1 hr. After that, further ramped to 100°C, at which the temperature was held for 1 hr to sublime the Pt(AcAc)₂. The reactor was cooled to room temperature. After that, it was ramped to 350°C in flow of air for 2 hr and calcined at that temperature to decompose the platinum precursor. Finally, the Pt/KL catalyst obtained was kept in a desiccator. The actual metal content was analyzed by AAS analysis.

Catalytic Activity Measurements: n-Octane Aromatization

The catalytic activity studies were conducted at atmospheric pressure in a 0.5 –inch glass tube with an internal K-type thermocouple for temperature measurement. The reactor was a single pass and continuous-flow type. 200 mg of catalysts was used in each run. Prior to reaction, the temperature was slowly ramped in flowing H₂ for 2 hr up to 500°C and in-situ reduced at that temperature for 1 hr. n-Octane was added by injection with a syringe pump. In all experiments, the hydrogen to n-octane molar ratio was kept at 6. The products were analyzed using a Shimadzu GC-17A equipped with a HP-PLOT/Al₂O₃ “S” Deactivated capillary column. The GC column temperature was programmed to obtain adequate products separation. The temperature was first kept constant at 40°C for 10 min, then it was linearly ramped to 195°C and held for 30 min.

Catalyst Characterization

1. *Diffuse Reflectance Infrared Fourier Transform Spectroscopy (DRIFTS)* of Adsorbed CO : The fresh Pt/KL and Pt/synthesized KL were characterized by DRIFTS using adsorbed CO as a probe in a Bruker Epuinox 55 spectrometer equipped with MCT detector. Experiments were performed in a diffuse reflectance cell from Harrick Scientific typed HVC-DR2, with ZnSe windows. For each IR spectrum, a background was collected on the sample reduced in situ under a flow of hydrogen at 300°C for 1 hr and purged in helium for 30 minutes at room temperature. Then, a flow of 5%CO in helium was sent over the sample for 30 min, followed by purging helium flow for 30 min. After this treatment, the spectrum of adsorbed CO was collected.

2. *Hydrogen Chemisorption* : H₂ uptake and degree of dispersion were determined by using pulse technique (Thermo Finnigan modeled TPDRO 1100). Prior to pulse chemisorption, the sample was reduced in H₂ atmosphere at 500°C for 1 hr. Then, the sample was purged with N₂ at 500°C for 30 min and cooled to 50°C in flowing N₂. A H₂ pulse (purge H₂, 0.4 ml) was injected into the sample at 50°C.

3. *Temperature Programmed Oxidation (TPO)* : Temperature programmed oxidation technique was employed to analyze the amount and characteristics of coke deposition on the spent catalysts. TPO of the spent catalysts was performed in a continuous flow of 2% O₂/He and the temperature was linearly increased with a heating rate of 12°C/min. The oxidation was conducted in a ¼” quartz fixed-bed reactor. The spent catalyst was dried at 110°C overnight before being weighed 30 mg of the dry sample was supported on a bed of

quartz wool. The sample was flushed by 2% O₂ in He for 30 min before the TPO was performed. The CO₂ produced by the oxidation of coke species was further converted to methane using a methanizing filled with 15% Ni/Al₂O₃ at 400°C. The methane was analyzed using an FID detector. The amount of coke was calibrated by using a 50 μl pulse of pure CO₂.

Results and Discussion

1. Synthesis of KL zeolite

1.1 Effects of ageing and crystallization times

In this work, the crystallization step was done by using microwave heating technique. The optimum ageing time and crystallization time were investigated. The ageing time and crystallization time were varied in the range of 0-30 hr and 20-35 hr, respectively. All samples were characterized by XRD to determine the crystal structure of KL zeolite, crystallinity, and purity of the sample. The XRD patterns of product obtained at different crystallization times with ageing time of 17 hr are shown in Fig. 1. It was found that at crystallization time of 20 hr (A17/C20/B1), the crystallinity was very low compared to the ones prepared with longer crystallization time. However, the zeolite prepared with 35 hr crystallization time (A17/C35/B1) exhibited undesired peak at $d=11.5 \text{ \AA}$ as shown in Fig. 1.

FTIR is another technique to confirm the crystallinity of the synthesized zeolites. The FTIR spectra of the synthesized zeolites prepared with different ageing times, amorphous aluminosilicate, and commercial KL are illustrated in Fig. 2. As previously reported [Joshi, 1990], the characteristic FTIR band of crystalline KL is at 620 cm^{-1} . At ageing time of 17 hr, the zeolite exhibited small peak at 620 cm^{-1} . As ageing time increased from 17 to 30 hr, the crystallinity increased.

Based on XRD results, the crystallinity of the synthesized zeolites prepared with various ageing and crystallization times were summarized in Fig. 3. It was found that at ageing time shorter than 15 hr, the crystalline KL was not observed. This indicated that 15 hr was too short to create enough nuclei species. At higher ageing time, crystalline KL were observed in the batch prepared with appropriate crystallization time e.g. A17/C30/B1, A24/C30/B1, and A30/C30/B1.

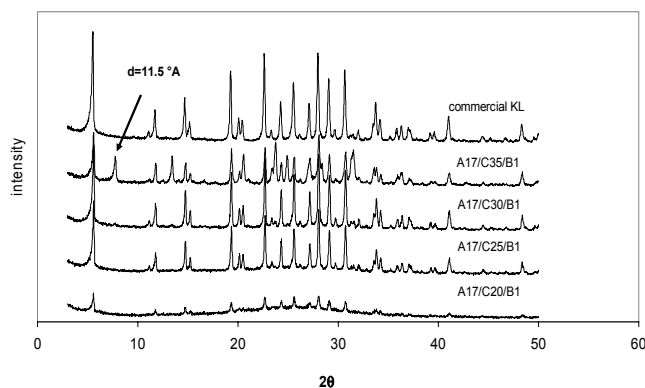


Fig. 1 XRD patterns of synthesized KL zeolite obtained with different crystallization times at crystallization temperature of 170°C and ageing time of 17 hr.

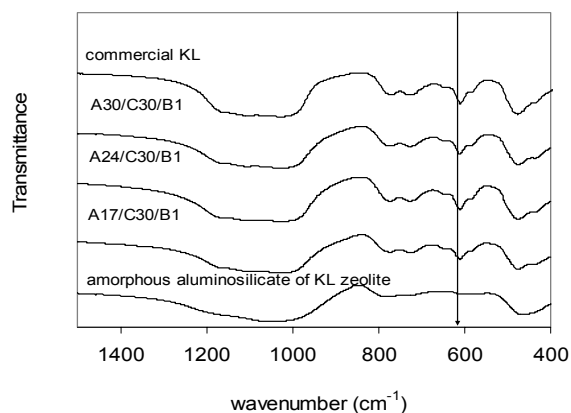


Fig. 2 FTIR spectra of synthesized KL zeolite obtained with different ageing time at crystallization time of 30 hr compared to amorphous KL zeolite.

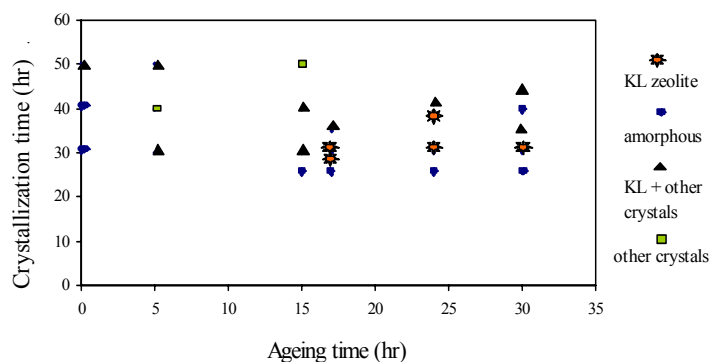


Fig. 3 Characteristic of products obtained with various ageing and crystallization times.

The Si/Al ratio, particle size, surface area, and pore volume, of all the synthesized and commercial KL zeolites were measured by XRF, DLS, and BET respectively. The results are listed in Table 1. It was found that the zeolite obtained with 24 hr ageing time resulted in smaller particle size than the one obtained with 17 hr ageing time. This result was in agreement with a previous study done by Ertl [Ertl et al., 1997]. They reported that the zeolite prepared with longer ageing time resulted in smaller crystal size. However, longer ageing time (30 hr) did not improve the reduction of the particle size of KL zeolite. However the particle sizes of synthesized zeolites are still larger by a factor of 3 compare to those of commercial KL. Also, the surface area and pore volume of synthesized KL zeolite are much less than those of commercial KL. XRF results showed that all synthesized KL zeolite has Si/Al ratio of 3.2-3.5 and the commercial has the ratio of 3.0. SEM photographs of the synthesized zeolites and commercial KL are shown in Fig.4. It was clearly seen that the synthesized KL zeolite are flat-cylindrical shape whereas the commercial KL are irregular sphere shape.

Table 1 List of zeolites and their analysis results.

Zeolite	Ageing time (hr)	Cryst. time (hr)	Ba (ppm)	Seeding (%)	Particle size (μm)	Surface area (m^2/g)	Pore volume (cm^3/g)	Si/Al
Commercial KL	n/a	n/a	n/a	n/a	0.53	302	0.206	3.0
A17/C30/B1	17	30	115	0.0	1.81	124	0.092	3.6
A24/C30/B1	24	30	115	0.0	1.47	144	0.093	3.3
A30/C30/B1	30	30	115	0.0	1.51	n/a	n/a	n/a
A24/C30/B2	24	30	330	0.0	1.63	147	0.122	n/a
A24/C30/B3	24	30	445	0.0	2.07	156	0.124	n/a
A24/C25/B1/S0.2	24	25	115	0.2	1.37	n/a	n/a	n/a
A24/C25/ B1/S0.5	24	25	115	0.5	1.37	n/a	n/a	n/a
A24/C25/ B1/S2.0	24	25	115	2.0	0.99	239	0.158	n/a
A24/C25/ B1/S5.0	24	25	115	5.0	0.94	228	0.171	2.93
A24/C25/ B1/S8.0	24	25	115	8.0	1.14	136	0.100	n/a

1.2 Effect of Barium

It has been reported that the formation of KL zeolite can be promoted by adding Ba [Verduijn, 1992]. In this report, the effect of barium on the formation of KL zeolite was also investigated. The amount of barium was varied from 0 to 445 ppm. The synthesis gel was aged for 24 hr and heated to 170°C for 30 hr for the crystallization process. All synthesized KL zeolites were characterized by FTIR. The results are shown in Fig. 5. The spectra showed that without Ba, the resultant did not show the zeolite characteristic band at 620 cm^{-1} . It was still amorphous aluminosilicate. However, when small amount of barium was added, the crystalline KL was observed. In addition, it was observed that the higher amount of barium resulted in the larger particle size as shown in Table 1. However, the surface area, pore volume, and Si/Al ratio were not significantly different among the zeolite prepared with different amount of Ba.

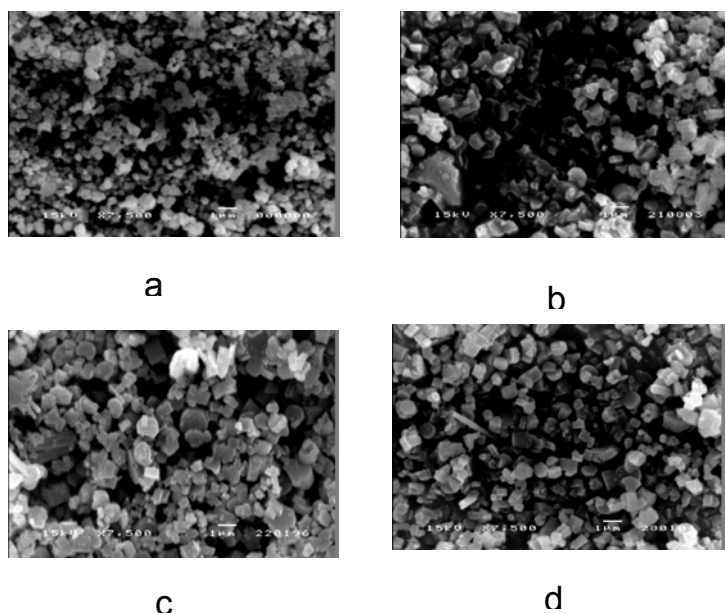


Fig. 4 SEM photographs of synthesized KL zeolite obtained with (a) commercial KL zeolite (b) ageing time of 17 hr and crystallization time of 30 hr (A17/C30/B1) (c) ageing time of 24 hr and crystallization time of 30 hr (A24/C30/B1) (d) ageing time of 30 hr and crystallization time of 30 hr (A30/C30/B1).

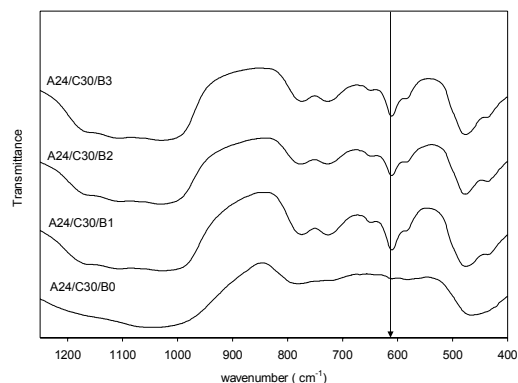


Fig. 5 FTIR spectra of synthesized KL zeolites obtained with the different amounts of barium at ageing time of 24 hr and crystallization time of 30 hr.

1.3 Effect of seeding

Seeding is the method that the small amount of zeolite is introduced to the synthesis gel, typically just right before the crystallization step in order to direct the crystallization towards a given zeolite and control the size of the final crystals. Seeding can increase the crystallization rate resulting in the shorter time of crystallization. For the reduction of the particle size of KL zeolite, the parameters that can be controlled are crystallization time and crystallization temperature. If zeolite is formed at lower temperature and shorter crystallization time, the particle size obtained should be smaller [Hincapie et al., 2004].

In this work, the commercial KL zeolite was used as seed. The amount of seed was varied from 0.0-8.0 wt%. The crystallization time was reduced from 30 hr to 25 hr. From

Table 1, it was found that the seed in the range of 2.0-5.0 wt% resulted in smaller crystal compared to other synthesized zeolites. Compared to zeolite without seeding at crystallization time of 30 hr, the addition of seed resulted in the reduction of the crystal size to 1 micron. If the amount of seed was too low or too high, the particle sizes of KL zeolites were increased. The low amount of seed was not enough to induce the gel to grow on the surface of seed with the crystallization time of 25 hr. The higher amount of seed (8.0 wt%) may have too much impurity for crystallization, and this will increase the crystallization rate resulting in larger crystal size. The SEM pictures are shown in Fig. 6.

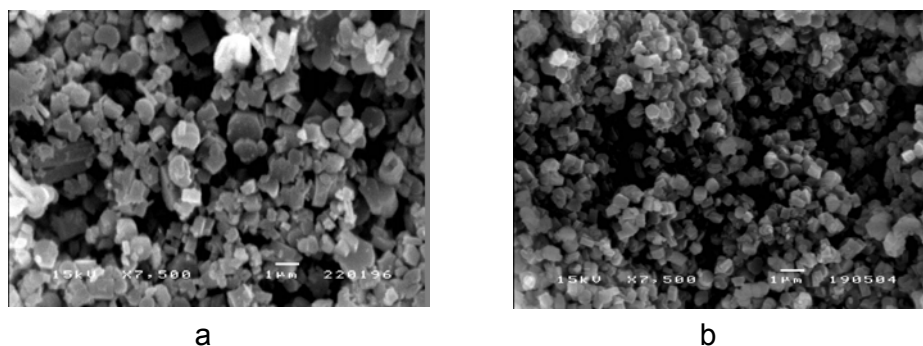


Fig. 6 SEM photographs of synthesized KL zeolite obtained with (a) 0% seeding and (b) 5% seeding.

2. Characterization of Pt/KL catalysts

2.1 Diffuse reflectance infrared Fourier transform spectroscopy (DRIFTS) of adsorbed CO

The Pt supported on A17/C30/B1, A24/C30/B1, A24/C30/B3, A24/C25/B1/S5.0, and commercial KL were analyzed by FTIR of adsorbed CO. This technique has been utilized to investigate size and location of Pt clusters in L zeolite [Jacobs et al., 2001]. The typical FTIR measurement for Pt/KL exhibited the bands between 2150 and 1900 cm^{-1} . The band below 2050 cm^{-1} represents Pt clusters located inside the channels of the L zeolite. The band between 2050 cm^{-1} and 2075 cm^{-1} corresponds to larger Pt cluster in the pore mouth of the L zeolite, while the bands above 2075 cm^{-1} are due to Pt clusters located outside the zeolite pore. The DRIFTS spectra of Pt/commercial KL, Pt/A17/C30, Pt/A24/C30/B1, Pt/A24/C25/B1/S5.0, and Pt/A24/C30/B3 are shown in Fig. 7. These results indicated that Pt/A17/C30/B1, Pt/A24/C30/B1, and Pt/A24/C25/B1/S5.0 have the Pt clusters located near the pore and inside the pore channel of KL zeolite. In contrast, most of Pt cluster are located inside the pore channel of KL zeolite in the Pt/commercial KL and Pt/A24/C30/B3. The location of Pt cluster loading on the flat-cylinder KL zeolite is dependent on the particle size of KL zeolite. The larger the particle size of KL zeolite, the larger fraction of Pt inside the pore channel of KL zeolite. However, the location of Pt cluster loading on the commercial KL zeolite, which is the smallest particle size of KL, is inside the pore channel of KL zeolite. From these results, it can be concluded that not only the particle sizes of KL zeolites affect on the location of Pt cluster, but also the morphologies of them does.

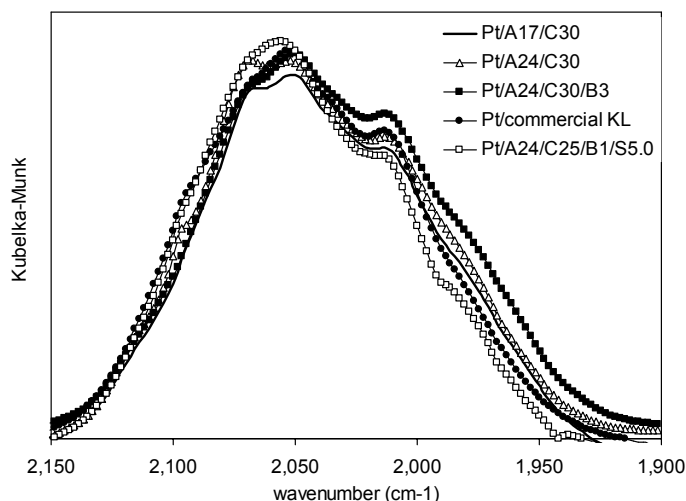


Fig. 7 DRIFTS spectra of CO adsorbed on Pt/commercial KL, Pt/A17/C30/B1, Pt/A24/C30/B1, and Pt/A24/C30/B3 catalysts.

2.2 Hydrogen Chemisorption

The Pt catalysts with various supports were tested for Pt dispersion by hydrogen chemisorption technique. The Pt dispersions in term of H/Pt ratio after reduction at 500°C are reported in Table 2. Most of the catalysts gave the ratio of H/Pt higher than one, indicating very high dispersion. Pt/A24/C30 showed the lowest Pt dispersion.

Table 2 Characterization data of fresh and spent catalysts.

Catalysts	Pt content (wt%)	H/Pt after reduction at 500°C	Coke deposit after rxn with n-C8 for 550 min. (wt %)
Pt/commercial KL	0.98	1.48	2.50
Pt/A17/C30/B1	0.96	1.15	0.83
Pt/A24/C30/B1	0.94	0.79	0.76
Pt/A24/C30/B3	0.94	1.04	1.35
Pt/A24/C25/B1/S5.0	1.06	1.12	1.65

3. Catalytic activity measurements: n-octane aromatization

The prepared Pt/KL catalysts with different supports were tested for the activity of n-octane aromatization. The conversion, selectivity to total aromatics, and selectivity to C8 aromatics are shown in Fig. 8a, 8b, and 8c respectively. At 10 min time on stream, the n-octane conversions are almost 100% for all catalysts. However, these catalysts deactivated quickly due to coke deposit [Jongpatiwut et al., 2003]. It was found that Pt/A17/C30/B1,

Pt/A24/C30/B1, and Pt/A24/C25/B1/S5.0 catalysts deactivated faster than Pt/commercial KL and Pt/A24/C30/B3.

The spent catalysts were analyzed by temperature program oxidation (TPO) for quantify the amount of coke deposit after reaction with n-octane for 550 min. The results are summarized in Table 2. The results showed that the amounts of coke deposit on Pt/A17/C30/B1 and Pt/A24/C30/B1 were much less than that on Pt/A24/C30/B3 and Pt/commercial KL.

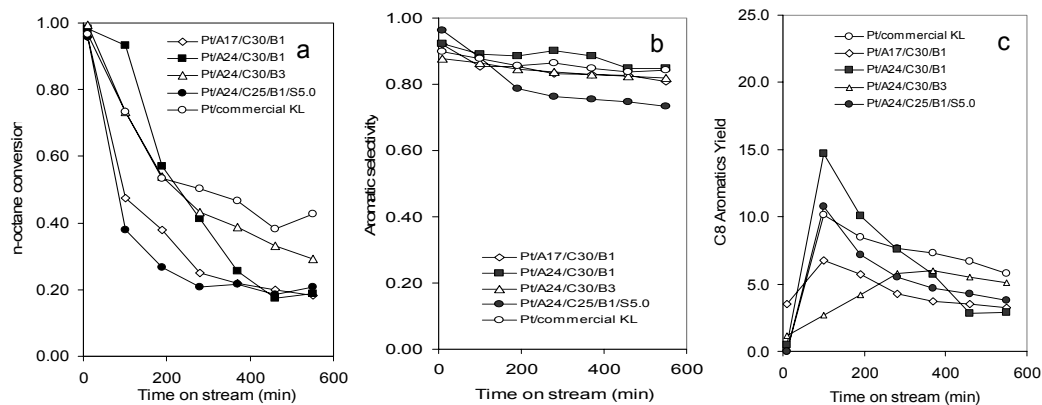


Fig. 8 The variation of (a) n-octane conversion (b) total aromatics (c) C8 Aromatics Yield (%) with time on stream of Pt/KL catalysts at 500°C , WHSV 5 hr⁻¹, and H₂/HC:6.

Since the Pt clusters of Pt/commercial KL and Pt/A24/C30/B3 were inside the pore channel of KL zeolite compared to other catalysts having Pt clusters near the pore mouth and inside the pore. When the coke deposited on the catalyst, the Pt clusters near the pore mouth may block the pore of zeolite easier than Pt inside the pore of KL zeolite. When the pore was blocked, the reactant cannot get into the pore of zeolite resulting in drastic drop in conversion. The results correspond to the small amount of coke deposit on the Pt/A17/C30, and Pt/A24/C30 compared to the coke deposition on Pt/A24/C30/B3 and Pt/commercial KL., Fig. 8b shows aromatic selectivity of those catalysts. The results indicated that all catalysts exhibited similar total aromatics selectivity. However, all catalysts resulted in low total C8 aromatic yields (ethylbenzene (EB), o-xylene (OX)) as shown in Fig. 8 (c), especially on the Pt/A24/C30/B3 which is the largest particle size of supported KL zeolite. The data indicated that the particle size of KL zeolite has the effect on the EB and OX yield.

Fig. 9a and b show the evolution of EB/OX as a function of time on stream and function of particle size, respectively. It was observed that the ratio increased with time on stream. Since the critical size of OX (0.76 nm) is larger than EB (0.67 nm), so OX diffuses through the pore of KL zeolite slower than EB. The increase in ratio with time on stream has been reported in our previous work [Jongpatiwut et al., 2003]. This is because once the coke started deposit and block the pore, it made more difficult for OX to get out of the pore compared to EB. In Fig. 9b, it was clearly seen that the EB/OX ratio increased with the crystal size of zeolite. This proved the hypothesis that the longer pore of zeolite has more restriction for OX to escape the pore.

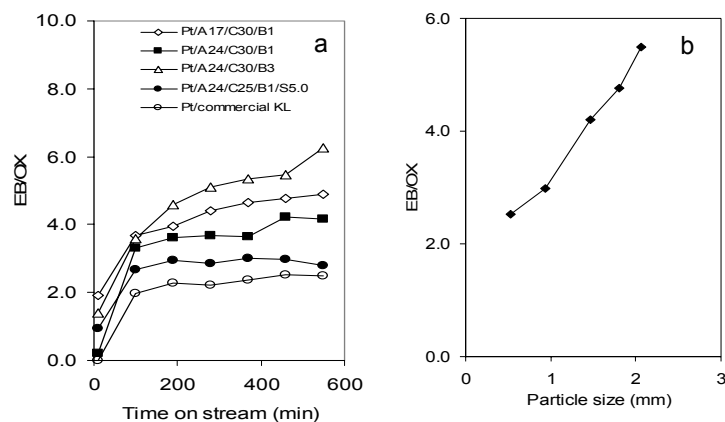


Fig. 9 (a) The variation of EB/OX obtained from different Pt/KL catalysts as a function time on stream (b) Re-plot the data at 460 min time on stream as a function of particle size of zeolites. Reaction condition: 500°C, WHSV 5 hr⁻¹, and H₂/HC: 6.

Conclusions

In the synthesis of KL zeolite by microwave technique, ageing time, amount of Ba and amount of seeding had an effect to the crystallinity and crystal size of the resultant zeolites. It was found that the longer ageing time, the higher the amount of nuclei, resulting in the smaller size of crystal. Nevertheless, the size of KL zeolite was increased with amount of Ba. In addition, proper amount of seeding could reduce the crystal size by increasing crystallization rate at a shorter crystallization time. For the catalytic performance, it was found that the crystal size had a great effect on EB/OX ratio. The larger particle size gave higher EB/OX ratio due to more restriction for OX to diffuse through the zeolite pore. Finally, in order to maximize C8-aromatics by avoiding secondary hydrogenolysis, the synthesis of zeolite with shorter pore length is required.

Acknowledgements

This research was supported by the Petroleum and Petrochemical College of Chulalongkorn University, the Thailand Research Fund and Ratchadapiseksomphot Endowment of Chulalongkorn University. We would like to acknowledge Oklahoma Center for Advancement of Science and Technology (OCAST) for financial support of the work that has been done at the University of Oklahoma.

Literature Cited

- Arika, J., Itabashi, K., and Tamura, Y., Process for preparation of L type zeolites, US Pat. 4 530 824, 1985.
- Chu, P., Dwyet, F.G., and Vartuli, J.C., Crystallization method employing microwave radiation, US Pat. 4 778 666, 1998.
- Ertl, G., Knozinger, H., and Weitkamp, J. Handbook of Heterogeneous Catalysis, 1, 313, 1997.
- Hincapie, B.O., Garces, L.J., Ahang, Q., Sacco, A., and Suib, S.L., Synthesis of mordenite nanocrystals, Micropor. Mesopor. Mater., 67, 19-26, 2004.

- Jacobs, G., Alvarez, W.E., and Resasco, D.E., Study of preparation and parameters of powder and palletized Pt/KL catalysts for n-hexane aromatization, *Appl. Catal. A*, 206, 267-282, 2001.
- Jongpatiwut, S., Sackamduang, P., Osuwan, S., Rirksomboon, T., and Resasco, D.E., n-octane aromatization on a Pt/KL catalyst prepared by vapor-phase impregnation, *J. Catal.*, 218, 1-11, 2003.
- Joshi, P.N., Kotasthane, A.N., and Shiralkar, V.P., Crystallization kinetics of zeolite LTL, *Zeolites*, 10, 598-602, 1990.
- Meriaudeau, P., and Naccache, C., Dehydrocyclization of alkanes over zeolite-supported metal catalysts, *Catal. Rev.-Sci. Eng.*, 39 (1&2), 3-48, 1997.
- Romero, M.D. Gomez, J.M., Ovejero, C., and Rodriguez, A., Synthesis of LSX zeolite by microwave heating, *Mater. Res. Bull.*, 39, 389-400, 2004.
- Treacy, M.M.J., Pt agglomeration and entombment in single channel zeolites : Pt.LTL, *Micropor. Mesopor. Mater.*, 28, 271-292, 1999.
- Verduijn, J.P., Improved zeolite L, *Eur Pat. Appl.* 219 354, 1987.
- Verduijn, J.P., Mertens, M.M., and Antanis, M.H., Zeolites and processes for their manufacture, *US Pat.* 6 258 991 B1, 2001.
- Verduijn, J.P., Zeolite L, *Int. Pat.* WO 91/06367, 1991.
- Wortel, T.M., Zeolite L with cylindrical morphology, *US Pat.* 4 544 539, 1985.